

UCLA

UCLA Previously Published Works

Title

Abcc6 Deficiency Causes Increased Infarct Size and Apoptosis in a Mouse Cardiac Ischemia-Reperfusion Model

Permalink

<https://escholarship.org/uc/item/48x0w2nb>

Journal

Arteriosclerosis Thrombosis and Vascular Biology, 31(12)

ISSN

1079-5642

Authors

Mungrue, Imran N
Zhao, Peng
Yao, Yucheng
et al.

Publication Date

2011-12-01

DOI

10.1161/atvbaha.111.237420

Peer reviewed

Abcc6 Deficiency Causes Increased Infarct Size and Apoptosis in a Mouse Cardiac Ischemia-Reperfusion Model

Imran N. Mungrue, Peng Zhao, Yucheng Yao, Haijin Meng, Christoph Rau, Jocelyn V. Havel, Theo G.M.F. Gorgels, Arthur A.B. Bergen, W. Robb MacLellan, Thomas A. Drake, Kristina I. Boström, Aldons J. Lusis

Objective—*ABCC6* genetic deficiency underlies pseudoxanthoma elasticum (PXE) in humans, characterized by ectopic calcification, and early cardiac disease. The spectrum of PXE has been noted in *Abcc6*-deficient mice, including dystrophic cardiac calcification. We tested the role of *Abcc6* in response to cardiac ischemia-reperfusion (I/R) injury.

Methods and Results—To determine the role of *Abcc6* in cardioprotection, we induced ischemic injury in mice in vivo by occluding the left anterior descending artery (30 minutes) followed by reperfusion (48 hours). Infarct size was increased in *Abcc6*-deficient mice compared with wild-type controls. Additionally, an *Abcc6* transgene significantly reduced infarct size on the background of a naturally occurring *Abcc6* deficiency. There were no differences in cardiac calcification following I/R, but increased cardiac apoptosis was noted in *Abcc6*-deficient mice. Previous studies have implicated the bone morphogenetic protein (BMP) signaling pathway in directing calcification, and here we showed that the BMP responsive transcription factors pSmad1/5/8 were increased in hearts of *Abcc6* mice. Consistent with this finding, BMP4 and BMP9 were increased and activin receptor-like kinase-2 and endoglin were downregulated in cardiac extracts from *Abcc6*-deficient mice versus controls.

Conclusion—These data identify *Abcc6* as a novel modulator of cardiac myocyte survival after I/R. This cardioprotective mechanism may involve inhibition of the BMP signaling pathway, which modulates apoptosis. (*Arterioscler Thromb Vasc Biol.* 2011;31:2806-2812.)

Key Words: ABC transporter ■ apoptosis ■ cardiovascular disease prevention ■ genetically altered mice ■ reperfusion injury

The ATP-binding cassette (ABC) transporters are a large family of membrane efflux transporters containing 48 members.¹ The substrate specificities of the ABC transporters are diverse and include lipids, peptides, polysaccharides, organic molecules, and ions. Based on sequence homology, *ABCC6* is most closely related to *ABCC1* and *ABCC2*, also known as multidrug resistance transporters, which transport a variety of substrates having importance for clinically relevant pharmaceutical agents.¹ The endogenous substrate for *ABCC6* is unknown.^{2,3}

ABCC6 mutations underlie the rare human disorder pseudoxanthoma elasticum (PXE).^{4,5} PXE is an autosomal recessive disease, characterized by ectopic mineralization of the skin, retina, and arteries, leading to the development of skin papules, blindness, and arterial sclerosis.⁶ Histologically, PXE is defined by elastic fiber calcification.⁷ *Abcc6* knockout mice have been generated on the C57BL/6 background and display parallel hallmarks of the human disease, suggesting

conserved mechanisms.^{8,9} Also, a naturally occurring mutation has been identified in several mouse strains, including C3H, which displays development of calcification consistent with PXE.¹⁰ Reports have shown that *Abcc6* is most abundantly expressed in liver and kidney,⁸ and recent parabiosis studies indicate that calcification in *Abcc6*-deficient mice is complemented by a circulating factor from wild-type mice.¹¹

There is evidence of early cardiac disease in PXE individuals deficient for *ABCC6*^{12,13} and population studies have identified the common Arg1141X mutation as associated with coronary artery disease in a Dutch population.^{14,15} We previously identified *Abcc6* genetic deficiency in the C3H mouse strain as the causative mutation conferring an increase in cardiac calcification.¹⁶ Cardiac calcification often accompanies cardiomyopathy and follows myocardial infarction, suggesting an overlapping etiology or related mechanism.¹⁷

We aimed to determine the effects of *Abcc6* deficiency in a mouse model of cardiac ischemia-reperfusion (I/R) injury,

Received on: June 2, 2011; final version accepted on: September 23, 2011.

From the Division of Cardiology and the Cardiovascular Research Laboratory, David Geffen School of Medicine (I.N.M., P.Z., Y.Y., H.M., J.V.H., W.R.M., K.I.B., A.J.L.) and Departments of Pathology (T.A.D.), Microbiology, Immunology, and Molecular Genetics (C.R., A.J.L.), and Human Genetics (C.R., A.J.L.), University of California, Los Angeles, CA; Department of Molecular Ophthalmogenetics, Netherlands Institute for Neuroscience (T.G.M.F.G., A.A.B.B.); Departments of Clinical Genetics (T.G.M.F.G., A.A.B.B.) and Ophthalmology (T.G.M.F.G., A.A.B.B.), Academic Medical Center, Amsterdam, the Netherlands. Current affiliation for Dr Meng: Pfizer Inc, Beijing, China.

Correspondence to Imran N. Mungrue, 675 Charles E. Young Dr S, MRL3210, Los Angeles, CA 90095. E-mail imungrue@yahoo.com

© 2011 American Heart Association, Inc.

Arterioscler Thromb Vasc Biol is available at <http://atvb.ahajournals.org>

DOI: 10.1161/ATVBAHA.111.237420

using the previously reported germline knockout and a naturally occurring *Abcc6*-deficient strain (C3H). Each model was compared with respective age-, sex-, and strain-matched controls replete for *Abcc6*. We also probed the mechanism linking *Abcc6* deficiency and the difference in infarct size following I/R, examining the transforming growth factor- β and bone morphogenetic protein (BMP) signaling pathways, and using terminal deoxynucleotidyl transferase dUTP nick-end labeling (TUNEL) staining to quantify apoptosis.

Methods

Cardiac I/R Injury and Infarct Size Analysis

All breeding, husbandry, and experiments with live animals were done in an approved vivarium, according to protocols defined by appropriate regulatory oversight. Ten- to 12-week-old mice (9 mice each for C57BL/6 versus B6-*Abcc6*-knockout [KO], and 10 mice per group for C3H versus C3H-*Abcc6*-transgenic [tg]) were anesthetized with sodium pentobarbital (70 mg/kg) intraperitoneal injection, placed on a heated mouse pad, and prepped for surgery. The neck was opened to visualize successful endotracheal intubation using a 10-mm plastic tube. Next, mice were placed on a minivent respirator, and left thoracotomy was performed to expose the heart. The left anterior descending coronary artery was occluded 2 mm below the left atrium, using a 2-mm section of PE-10 tubing and anchoring it in place with an 8-0 silk suture (Fine Science Tools). After 30 minutes of ischemia, the PE-10 tubing was removed, and flow was restored through the left anterior descending coronary artery. The chest was closed, and mice were allowed to recover on a warming pad. Mice were administered topical Buprenex as analgesic and monitored during the reperfusion period for overt signs of stress. After 48 hours reperfusion, mice were euthanized under anesthesia, and hearts were harvested. Evans blue dye was perfused via cannulation of the aorta, following religation of the left anterior descending coronary artery, to determine the area at risk (AAR), which was not stained blue. Hearts were frozen on dry ice, cut into 1-mm slices, and incubated with 1% 2,3,5-triphenyl-tetrazolium chloride (Sigma-Aldrich) in PBS at 37°C for 25 minutes. 2,3,5-Triphenyl-tetrazolium chloride stains viable tissue red, whereas infarcted area remains unstained. Heart slices were fixed with 10% formaldehyde (Fisher Scientific) in PBS overnight at 4°C. The infarct area (a), AAR (b), and total cross sectional left ventricle area (c) were determined via planimetry using ImageJ software (National Institutes of Health). Myocardial infarction size is reported as infarct area divided by AAR (a/b). Percentage AAR (b/c) was also determined to ensure equivalent cardiac ischemia between experimental groups. All surgeries and downstream analyses were done by operators blinded with respect to the genotype of mice.

Mice Used for Experiments

C57BL/6J (#000664) and C3H/HeJ (#000659) mice were purchased from the Jackson Laboratory. *Abcc6*-KO mice were provided by Dr Bergen⁸ and had been backcrossed for 10 generations on the C57BL/6 background. C3H-*Abcc6*-tg mice were previously reported¹⁶ and contain an *Abcc6* bacterial artificial chromosome transgene derived from C57BL/6. The C3H-*Abcc6*-tg allele had been back-crossed to the C3H/HeJ strain for >15 generations.

Western Blotting

Whole hearts were harvested in 10 mmol/L Hepes (pH 7), 2 mmol/L NaCl, 2 mmol/L CaCl₂, and 1.5% Triton X-100, plus phosphatase (2 mmol/L Na₃VO₄) and protease inhibitors (Sigma P8340), and protein determination was performed using the Bio-Rad Dc Assay. Protein samples were boiled following addition of Laemmli loading dye, separated on Invitrogen precast gels, and transferred to polyvinylidene difluoride membrane. Membranes were rinsed in 1×tris buffered saline with tween 20 (TBST) (#9997, Cell Signaling Technology), blocked in 5% skim milk-TBST for 1 hour at 23°C, rinsed in TBST, and incubated with primary antibodies diluted in 5%

skim milk-TBST or 3% bovine serum albumin-TBST for 1 hour at 23°C or overnight at 4°C. Membranes were then washed with TBST and incubated with secondary antibodies: anti-rabbit (KPL #474-1516) or anti-goat (sc-2056, Santa Cruz Biotechnology), diluted in 5% skim milk-TBST. Membranes were washed with TBST, and incubated with ECL Plus for detection and exposed to film or imaged using a Bio-Rad Chemidoc system.

Immunostaining

Fresh frozen sections were thawed, fixed in 3% paraformaldehyde/PBS, washed in PBS, and permeabilized with 0.2% Triton X-100/PBS for 5 minutes. Slides were incubated in blocking solution 5% goat serum in PBS with 0.1% Tween 20 for 30 minutes. Sections were incubated with primary antibody diluted in blocking serum for 1 hour at 23°C, followed by washes with PBS. Detection was done using an Alexa 488-conjugated anti-rabbit secondary antibody (Invitrogen A-11008) diluted in blocking buffer.

TUNEL Staining

Apoptosis quantification was done using the commercial Apoptag-RED TUNEL kit (#S7165, Chemicon) as previously reported.¹⁸ The number of TUNEL-positive cells was counted per low power field in $n=3$ mice per group, averaging 3 sections per mouse and 4 fields per section.

Antibodies Used for Immunoblotting and Immunostaining

pSmad1/5/8 (#9511, Cell Signaling Technology), pSmad2/3 (sc11769, Santa Cruz Biotechnology), panSmad (sc7153, Santa Cruz Biotechnology), CD31 (MAB1398, Millipore), BMP4 (sc6896, Santa Cruz Biotechnology), BMP9 (AF3209, R&D Systems), BMP2 (sc6895, Santa Cruz Biotechnology), BMP6 (sc7406, Santa Cruz Biotechnology), NKX2-5 (PAB14394, Abnova), activin receptor-like kinase (ALK)-2 (sc5671, Santa Cruz Biotechnology), endoglin (#3290, Cell Signaling Technology), ALK1 (sc19546, Santa Cruz Biotechnology), ALK3 (sc20736, Santa Cruz Biotechnology), ALK6 (sc25455, Santa Cruz Biotechnology), BMP receptor-II (AF811, R&D Systems), Matrix Gla protein (MGP) (ALK-804-512, Alexis Biochemicals), Smad4 (#9515, Cell Signaling Technology), Smad6/7 (sc7004, Santa Cruz Biotechnology), and troponin1 (sc15368, Santa Cruz Biotechnology).

Results

B6-*Abcc6*-KO Mice Have Larger Infarcts Following Cardiac Ischemia Reperfusion Injury Compared With Controls

To determine the contribution of *Abcc6* to cardioprotection, we examined cardiac infarct size following I/R injury. Wild-type C57BL/6 mice were compared with age-, sex-, and strain-matched mice having a targeted germline deletion of the *Abcc6* gene (B6-*Abcc6*-KO). Infarct size in B6-*Abcc6*-KO mice was increased by 30% compared with controls ($P<0.05$; Figure 1a). The AAR between these 2 groups of mice was not different, nor was baseline cardiac function (Supplemental Figures III and V, available online at <http://atvb.ahajournals.org>), indicating that the increased infarct size could not be explained by differences in perfusion or function in *Abcc6*-deficient mice.

Abcc6-Deficient C3H Mice Have Larger Infarcts Compared With C57BL/6, Which Is Rescued by *Abcc6* Overexpression

We next examined the effect of cardiac I/R injury in C3H mice that harbor a naturally occurring mutation rendering them *Abcc6* deficient.¹⁰ These mice were compared with

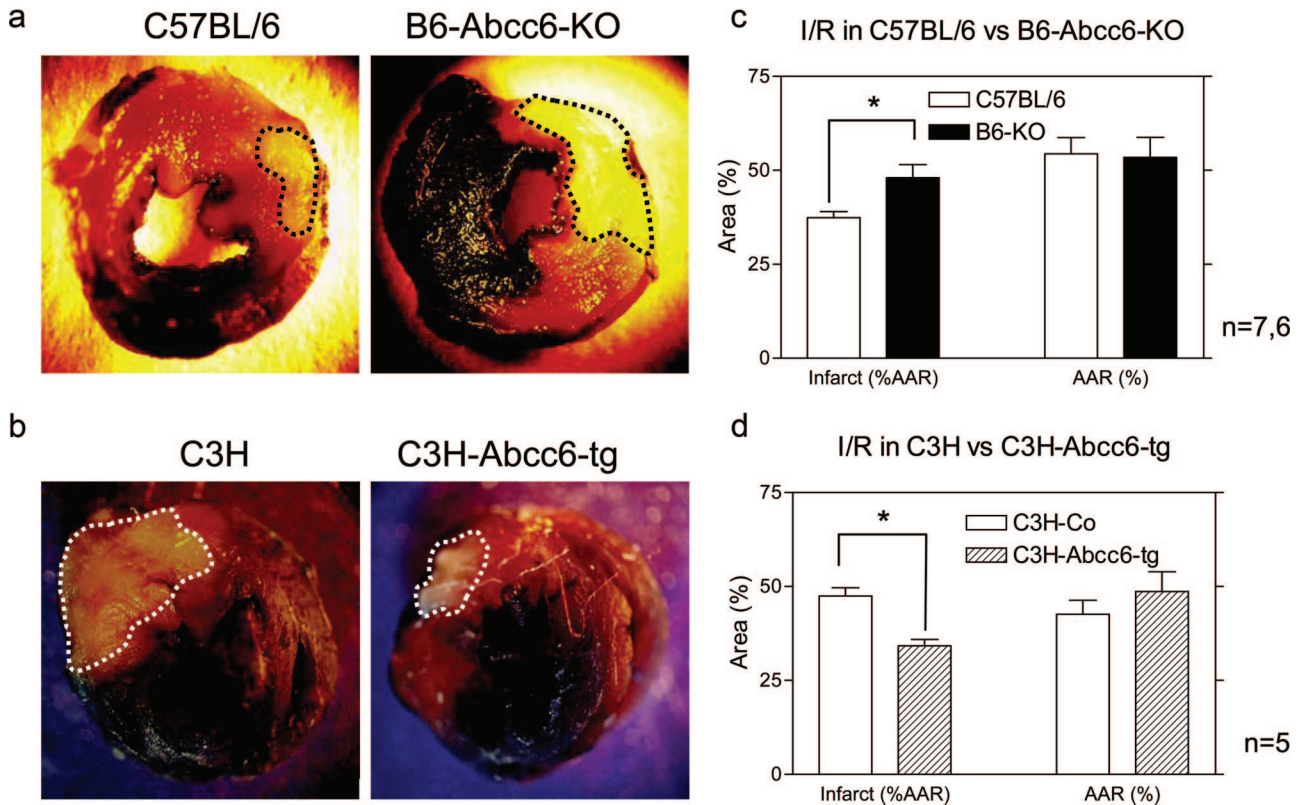
* $p < 0.05$ 

Figure 1. Increased infarcts in *Abcc6* deficiency following cardiac ischemia-reperfusion (I/R). **a** and **b**, Representative cardiac slices from C57BL/6 vs B6-*Abcc6*-knockout (KO) (**a**) and C3H (*Abcc6*-deficient) vs C3H-*Abcc6*-transgenic (tg) (**b**) mice following cardiac I/R injury. Infarcted area is outlined with dashed lines. **c** and **d**, Quantitation of infarcted area and area at risk (AAR) from C57BL/6 vs B6-*Abcc6*-KO ($n=7$ and 6) (**c**) and C3H (*Abcc6*-deficient) vs C3H-*Abcc6*-tg mice ($n=5$ each) (**d**). *Student *t* test $P < 0.05$, infarct size C57BL/6 vs B6-*Abcc6*-KO; $P < 0.05$, infarct size C3H vs C3H-*Abcc6*-tg.

age-, sex-, and strain-matched transgenic mice that have a complementing wild-type C57BL/6 bacterial artificial chromosome transgene (C3H-*Abcc6*-tg) under endogenous regulation. Cardiac infarct size in the C3H (*Abcc6*-deficient) strain was significantly increased compared with wild-type C57BL/6 mice (Figure 1b) and was similar to B6-*Abcc6*-KO as reported above. Furthermore, *Abcc6* proficient C3H-*Abcc6*-tg mice had a 30% decrease in cardiac infarct size compared with the C3H controls ($P < 0.05$; Figure 1b). The complementing C57BL/6 bacterial artificial chromosome transgene rescued the phenotype noted in *Abcc6*-deficient C3H mice, demonstrating that *Abcc6* is the major determinant of the susceptibility of the C3H strain to I/R injury. AAR and baseline cardiac function (Supplemental Figures IV and V) were not different between these 2 groups of mice. Collectively, these data demonstrate an important role for *Abcc6* in modulating cardiac injury after I/R, using 2 different strains of mice and reciprocal knockout and transgenic lines.

***Abcc6*-Deficient Mice Have Enhanced Cardiac Myocyte Apoptosis Following Ischemia Reperfusion Injury, But No Change in Cardiac Calcification**

Because apoptosis is a well-characterized mechanism that would contribute to adverse outcome following cardiac ischemia,¹⁹ we quantified TUNEL-positive nuclei in cardiac

sections from *Abcc6*-deficient B6-*Abcc6*-KO compared with age-sex matched controls. There was a 25-fold increase in the number of TUNEL-positive nuclei in the periinfarct area of the *Abcc6*-deficient strain versus the respective controls ($P < 0.05$; Figure 2). Given the previously reported role of *Abcc6* in regulating calcification, we performed histological staining on serial sections using our established method.¹⁶ There was no evidence of cardiac calcification in either the *Abcc6*-deficient strain or the control at the time point examined (48 hours postischemia) in 10- to 12-week-old mice. We also scored inflammatory cell infiltration in sections from *Abcc6*-deficient mice and noted increased cellularity that was consistent with the difference noted in infarct size.

***Abcc6*-Deficient Mice Have Increased Cardiac pSmad1/5/8, Indicative of BMP Pathway Activation**

Because previous reports show that *Abcc6*-deficient mice have increased circulating MGP levels, and there is a large body of data highlighting the role of transforming growth factor- β in cardiac I/R models,^{20–22} we examined the expression of pSmad2/3 and pSmad1/5/8 in cardiac extracts from *Abcc6*-deficient mice. Phosphorylation of Smad2/3 is primarily achieved downstream of activation by transforming growth factor- β ligands, whereas Smad1/5/8 is a target of BMPs. There was no difference in pSmad2/3 levels in hearts

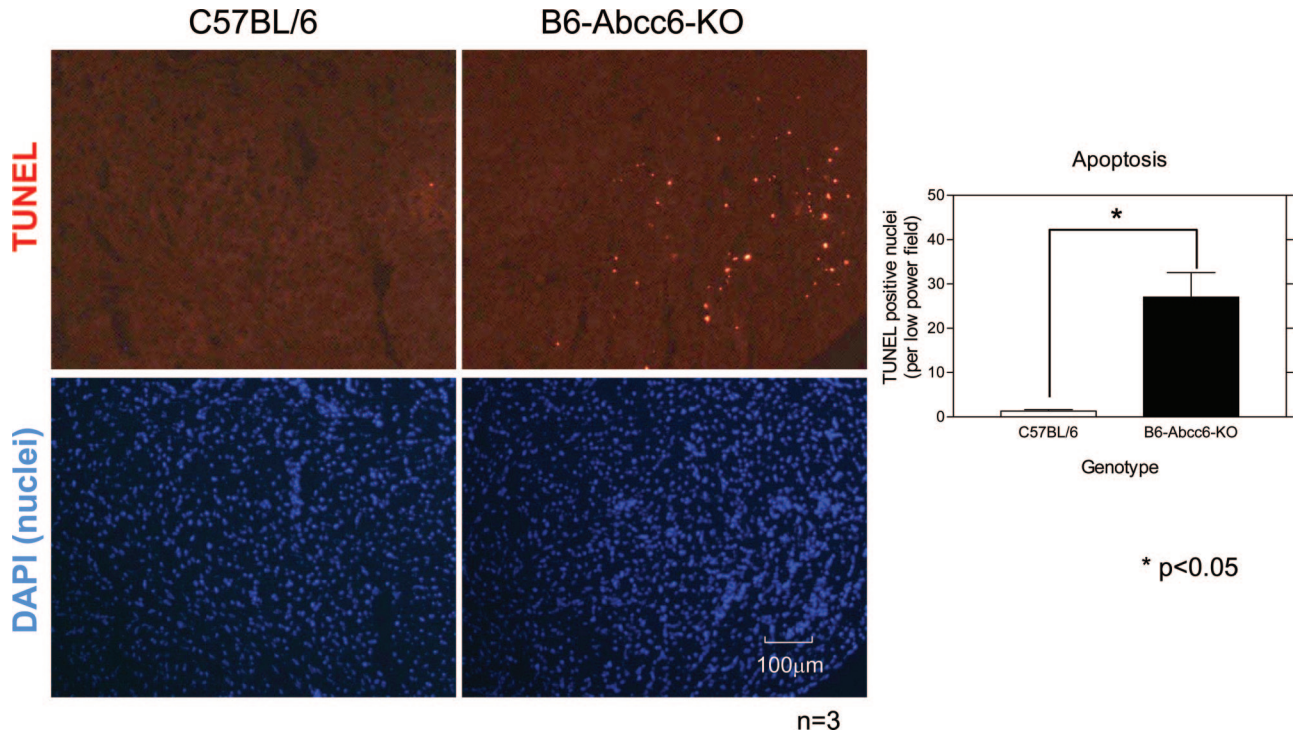


Figure 2. Increased apoptosis in B6-*Abcc6*-knockout (KO) hearts following ischemia-reperfusion (I/R). Representative cardiac sections were stained using the terminal deoxynucleotidyl transferase dUTP nick-end labeling (TUNEL) method (red), and 4',6-diamidino-2-phenylindole (DAPI) nuclear counterstain (blue) in C57BL/6 and *Abcc6*-deficient B6-*Abcc6*-KO mice. Quantification of TUNEL-positive nuclei is shown in the graph ($n=3$ each). *Student *t* test $P<0.05$.

of *Abcc6*-deficient mice; however, there was a 10-fold increase in pSmad1/5/8 (Figure 3a and Supplemental Figure I). To determine the cell type responsible for this increase, we examined ventricular sections from C57BL/6 versus B6-*Abcc6*-KO mice for pSMAD1/5/8 immunostaining after I/R (Figure 3b). The increased expression of pSMAD1/5/8 in B6-*Abcc6*-KO mice colocalized to nuclei of cardiac myo-

cytes costained with troponin and did not overlap with the vascular marker CD31 (Supplemental Figure II). These data demonstrate increased cardiac myocyte pSmad1/5/8, a central component of the BMP signaling axis, in *Abcc6* deficiency following cardiac I/R injury.

***Abcc6*-Deficient Mice Have Increased Cardiac BMP4 and BMP9 Expression, Along With Decreased ALK2, Endoglin, and Vascular MGP**

To determine the status of signaling pathways associated with pSMAD1/5/8, we examined the expression of several BMP ligands (BMP2, BMP4, BMP6, BMP7, BMP9, and BMP10) and receptors (ALK1, ALK2, ALK3, ALK6, BMP receptor-II, and endoglin) in cardiac extracts from *Abcc6*-deficient mice and wild-type controls. We noted a significant increase in cardiac expression of BMP4 and BMP9 (Figure 4) and downregulation of ALK2 and endoglin (Figure 4) in mice deficient for *Abcc6* compared with controls. Quantifications of Western blots are reported in Supplemental Figure I. BMP4 and BMP9 were increased 1.5- and 2-fold, and ALK2 and endoglin were reduced 0.6- and 0.5-fold, in *Abcc6*-deficient versus control. We also examined the expression of the common coactivator Smad4 and inhibitory Smad6 and Smad7 and noted no change in expression in cardiac extracts from *Abcc6*-deficient mice versus controls (data not shown).

We also examined expression of the BMP antagonist MGP by immunostaining in cardiac sections from C57BL/6 versus B6-*Abcc6*-KO mice subjected to I/R (Figure 5). Interestingly, we noted dramatically reduced expression of MGP in *Abcc6* deficiency. The staining pattern for MGP was similar to that

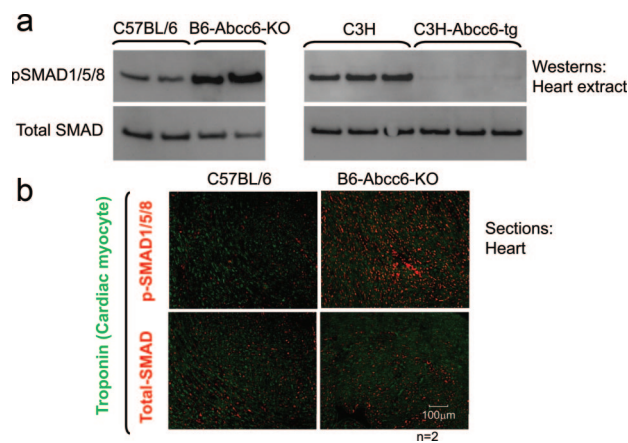


Figure 3. Increased bone morphogenetic protein (BMP) signaling in *Abcc6* deficiency. **a**, Expression of pSmad1/5/8 and panSmad by Western blot in cardiac extracts from *Abcc6*-deficient mice (B6-*Abcc6*-knockout [KO] and C3H) and the respective replete controls (C57BL/6 and C3H-*Abcc6*-transgenic [tg]). C57BL/6 vs B6-*Abcc6*-KO, $n=2$; C3H vs C3H-*Abcc6*-tg, $n=3$ each. **b**, Immunostaining of remote zone cardiac sections from B6-*Abcc6*-KO vs C57BL/6 controls to detect pSmad1/5/8 (red, top) or panSmad (red, bottom) and the cardiac myocyte marker troponin (green), $n=3$ each.

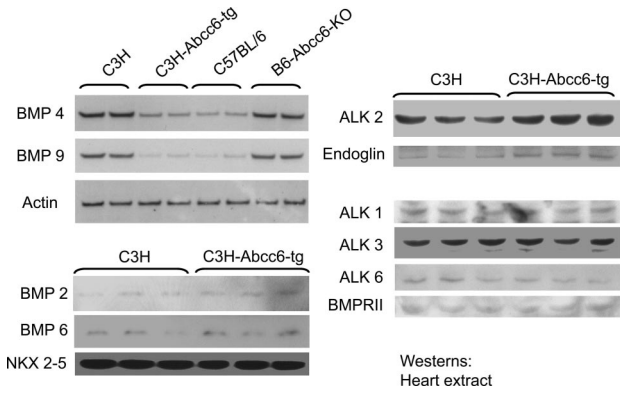


Figure 4. Increased bone morphogenetic protein 4 (BMP4) and BMP9 and decreased ALK2 and endoglin in cardiac extracts from *Abcc6*-deficient mice. Expression of BMP4, BMP9, BMP2, BMP6, NKX2-5, ALK2, endoglin, ALK1, ALK3, ALK6, and BMP receptor-II, by Western blot, in cardiac extracts from *Abcc6*-deficient mice (C3H) and controls (C3H-*Abcc6*-transgenic [tg]), $n > 3$ per group. BMP4 and BMP9 expression is also shown for C57BL/6 and B6-*Abcc6*-knockout (KO), $n = 2$.

for CD31, an endothelial cell marker, suggesting that the normal endothelium, or basement membrane, expression was reduced in the setting of *Abcc6* deficiency. Taken with the enhanced pSMAD1/5/8 noted above, these data imply dysregulation of specific BMP signaling pathways in *Abcc6*-deficient hearts.

Discussion

ABCC6 is expressed mainly in liver and kidney, and phenotypes associated with PXE appear to be complemented by a circulating factor¹¹; thus, restoration of the natural substrate of ABCC6 may be of clinical benefit in the setting of PXE.²³ Although *Abcc6*-deficient mice do not develop myocardial infarction, as noted in some patients with PXE, the data herein demonstrates a significant increase in infarct size using the mouse model subjected to cardiac I/R. This was accompanied by an increased inflammatory infiltrate but no change in cardiac calcification or perfusion, reflected by a similar region at risk following I/R, and no change in baseline cardiac function as determined by echocardiography. Our results suggest that the substrate of ABCC6 may have a wider therapeutic value, including broader use in the setting of myocardial infarction. Importantly, the consequences of *Abcc6* deficiency on adverse outcomes following cardiac I/R may occur at the level of the cardiac myocyte, which is a novel mechanism, in addition to previously defined roles in arterial sclerosis.^{12,14,24}

The frequency of PXE is $\approx 1/25\ 000$, and in population studies, the *ABCC6* Arg1141X mutant haplotype has been observed in 1.5% of individuals.¹⁴ Arg1141X homozygous mutations account for $\approx 25\%$ of PXE cases in the same population.²⁵ Collectively, *ABCC6* minor allele frequencies are below the cutoff of $\approx 5\%$ used in most Genome Wide

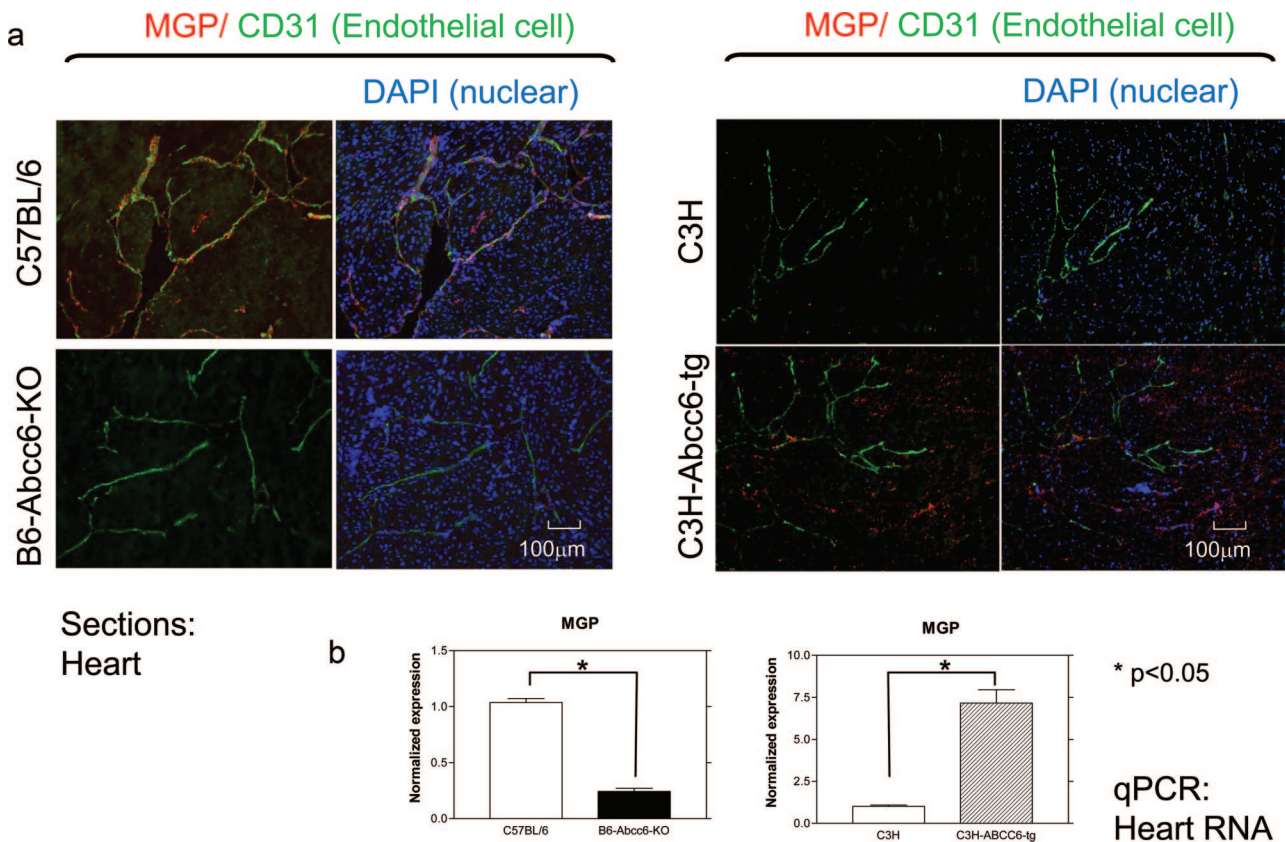


Figure 5. MGP detection by immunostaining in cardiac sections following ischemia-reperfusion (I/R) and quantitative polymerase chain reaction (qPCR). **a**, Immunostaining for MGP (red) and endothelial cell CD31 (green) in the remote region of cardiac sections from C57BL/6 vs B6-*Abcc6*-knockout (KO) mice subjected to I/R, $n = 3$ per group, and C3H vs C3H-*Abcc6*-transgenic (tg), $n = 2$. 4',6-Diamidino-2-phenylindole (DAPI) counterstain to visualize nuclei (blue) is shown in right panels. **b**, qPCR detection of MGP RNA expression in cardiac RNA from *Abcc6*-deficient C3H mice and controls, $n = 3$, and C57BL/6 vs B6-*Abcc6*-KO, $n = 3$. *Student *t* test $P < 0.05$.

Association Studies; however, our data suggest that a broader examination of *ABCC6* polymorphisms in cardiovascular disease is warranted. We hypothesize that *ABCC6* mutations contribute to an increased propensity for cardiovascular disease with aging in heterozygotes based on defects in vascular as well as cardiac myocytes. These data imply that studying the effects of *Abcc6* deficiency on cardiac myocyte function may be of importance especially because of the correlation between coronary artery disease and *ABCC6* polymorphism as previously reported,^{14,15} along with absence of association with incidence of stroke.¹⁵

We noted increased apoptosis in hearts of *Abcc6*-KO mice following cardiac I/R, accompanied by increased BMP4 and BMP9 and downregulation of ALK2 and endoglin. BMP4 is proapoptotic when administered to cardiomyocytes²⁶ and BMP9 to PC-3 cells.²⁷ Apoptosis accompanies ALK2 deficiency,²⁸ whereas endoglin expression can prevent apoptosis.²⁹ Collectively, these data imply that the end result of *Abcc6* deficiency on the heart is a perturbation of the BMP signaling pathway and increased propensity for apoptosis, an established mechanism that would lead to poor outcome following ischemia and contribute to heart failure.¹⁹

These data also support involvement of the BMP signaling pathway, via SMAD1/5/8 phosphorylation, as being important in cardioprotection. GDF5-KO (a BMP-related ligand) mice have been shown to develop larger infarcts following left anterior descending coronary artery occlusion, with associated increase in cardiac pSmad1/5/8.³⁰ Interestingly, BMP4 het-KO mice had smaller infarcts and decreased apoptosis following I/R, which was accompanied by decreased pSmad1/5/8 and blocked by BMP inhibitors.²⁶ These data point to a consistent role for increased cardiac pSmad1/5/8 expression as being detrimental in cardiac I/R or myocardial infarction, and this complex pathway represents an emerging area of study in the setting of cardioprotection.

Components of the BMP pathway altered in *Abcc6*-deficient mice play roles in cardiac morphogenesis,^{31–38} differentiation from embryonic stem cells,^{36,39–41} and myocardial infarction.²⁶ ALK2 genetic mutations in mice lead to congenital heart defects.^{42,43} Endoglin mutations underlie type 1 hereditary hemorrhagic telangiectasia in humans characterized by the presence of arteriovenous malformations (arterial-venous connections lacking connecting capillaries),⁴⁴ and display high output cardiac failure likely secondary to liver arteriovenous malformations.⁴⁵ Although plasma MGP levels are decreased in *Abcc6*-deficient mice⁴⁶ and humans with PXE,⁴⁷ plasma MGP levels are increased in humans with ischemic heart disease,⁴⁸ and an MGP polymorphism may be associated with plaque calcification and myocardial infarction.⁴⁹ Collectively, the data herein suggest complex roles for ligands and receptors of the BMP pathway in affecting cardiac physiology and contributing to adverse outcome following I/R accompanying *Abcc6* deficit.

The BMP signaling cascade plays diverse roles in development, and the hallmark of this pathway is induction of osteoblast differentiation, which is important for bone formation.⁵⁰ Although we did not see cardiac calcification at the time point examined (48 hours post-ischemia) in 10- to 12-week-old mice, our previous reports show that *Abcc6*-

deficient mice develop cardiac calcification following 4 weeks of treatment with a high-phosphate diet or with aging (12 months old).¹⁶ Importantly, these data implicate the shared BMP signaling mechanism as underlying the correlation between outcomes following myocardial infarction and cardiac calcification, and they suggest that further study may provide insight. Additionally, this work suggests that examining the BMP pathway may be of importance in the study of PXE, as a mechanism to explain ectopic calcification of arteries, retina, and skin noted in this human disease.

Our data highlight the contribution of *Abcc6* gene deficiency in cardiac I/R injury. Increased apoptosis resulting from deregulation of the BMP signaling pathway, evidenced by increased pSMAD1/5/8, is implicated as the molecular mechanism of this phenotype. Future studies examining these complex pathways may lead to important clinical therapeutic benefit. This work highlights the testable hypothesis examining the role of the natural substrate of *ABCC6*, when identified, in ameliorating adverse effects of myocardial infarction.

Sources of Funding

This work was supported by funding from the National Institutes of Health, Grants HL30568 (to A.J.L. and K.I.B.), HL81397 (to K.I.B.), and 5K99HL094709-02 (to I.N.M.), and the American Heart Association, Western Affiliate and National Center (to K.I.B.).

Disclosures

None.

References

- Dean M. *The Human ATP-Binding Cassette (ABC) Transporter Superfamily*. NCBI Bookshelf, National Library of Medicine, National Institutes of Health; 2002. Bookshelf ID: NBK31. <http://www.ncbi.nlm.nih.gov/books/nbk31/>.
- Madon J, Hagenbuch B, Landmann L, Meier PJ, Stieger B. Transport function and hepatocellular localization of mrp6 in rat liver. *Mol Pharmacol*. 2000;57:634–641.
- Ilias A, Urban Z, Seidl TL, Le Saux O, Sinko E, Boyd CD, Sarkadi B, Varadi A. Loss of ATP-dependent transport activity in pseudoxanthoma elasticum-associated mutants of human *ABCC6* (MRP6). *J Biol Chem*. 2002;277:16860–16867.
- Bergen AA, Plomp AS, Schuurman EJ, Terry S, Breuning M, Dauwerse H, Swart J, Kool M, van Soest S, Baas F, ten Brink JB, de Jong PT. Mutations in *ABCC6* cause pseudoxanthoma elasticum. *Nat Genet*. 2000; 25:228–231.
- Le Saux O, Urban Z, Tschuch C, Csiszar K, Bacchelli B, Quagliano D, Pasquali-Ronchetti I, Pope FM, Richards A, Terry S, Bercovitch L, de Paeppe A, Boyd CD. Mutations in a gene encoding an ABC transporter cause pseudoxanthoma elasticum. *Nat Genet*. 2000;25:223–227.
- Chassaing N, Martin L, Calvas P, Le Bert M, Hovnanian A. Pseudoxanthoma elasticum: a clinical, pathophysiological and genetic update including 11 novel *ABCC6* mutations. *J Med Genet*. 2005;42:881–892.
- Uitto J, Boyd CD, Lebwohl MG, Moshell AN, Rosenbloom J, Terry S. International centennial meeting on pseudoxanthoma elasticum: progress in PXE research. *J Invest Dermatol*. 1998;110:840–842.
- Gorgels TG, Hu X, Scheffer GL, van der Wal AC, Toonstra J, de Jong PT, van Kuppevelt TH, Levelt CN, de Wolf A, Loves WJ, Scheper RJ, Peek R, Bergen AA. Disruption of *Abcc6* in the mouse: novel insight in the pathogenesis of pseudoxanthoma elasticum. *Hum Mol Genet*. 2005; 14:1763–1773.
- Klement JF, Matsuzaki Y, Jiang QJ, Terlizzi J, Choi HY, Fujimoto N, Li K, Pulkkinen L, Birk DE, Sundberg JP, Uitto J. Targeted ablation of the *abcc6* gene results in ectopic mineralization of connective tissues. *Mol Cell Biol*. 2005;25:8299–8310.
- Aherrahrou Z, Doehring LC, Ehlers EM, Liptau H, Depping R, Linselnitschke P, Kaczmarek PM, Erdmann J, Schunkert H. An alternative

- splice variant in *Abcc6*, the gene causing dystrophic calcification, leads to protein deficiency in C3H/He mice. *J Biol Chem*. 2008;283:7608–7615.
11. Jiang Q, Oldenburg R, Otsuru S, Grand-Pierre AE, Horwitz EM, Uitto J. Parabolic heterogenetic pairing of *Abcc6*^{-/-}/*Rag1*^{-/-} mice and their wild-type counterparts halts ectopic mineralization in a murine model of pseudoxanthoma elasticum. *Am J Pathol*. 2010;176:1855–1862.
 12. Nolte KB. Sudden cardiac death owing to pseudoxanthoma elasticum: a case report. *Hum Pathol*. 2000;31:1002–1004.
 13. Leftheriotis G, Abraham P, Le Corre Y, Le Saux O, Henrion D, Ducluzeau PH, Prunier F, Martin L. Relationship between ankle brachial index and arterial remodeling in pseudoxanthoma elasticum. *J Vasc Surg*. 2011.
 14. Trip MD, Smulders YM, Wegman JJ, Hu X, Boer JM, ten Brink JB, Zwinderman AH, Kastelein JJ, Feskens EJ, Bergen AA. Frequent mutation in the *ABCC6* gene (R1141X) is associated with a strong increase in the prevalence of coronary artery disease. *Circulation*. 2002;106:773–775.
 15. Koblos G, Andrikovics H, Prohazska Z, Tordai A, Varadi A, Aranyi T. The R1141X loss-of-function mutation of the *ABCC6* gene is a strong genetic risk factor for coronary artery disease. *Genet Test Mol Biomarkers*. 2010;14:75–78.
 16. Meng H, Vera I, Che N, Wang X, Wang SS, Ingram-Drake L, Schadt EE, Drake TA, Lusis AJ. Identification of *Abcc6* as the major causal gene for dystrophic cardiac calcification in mice through integrative genomics. *Proc Natl Acad Sci U S A*. 2007;104:4530–4535.
 17. Bloom S, Peric-Golia L. Geographic variation in the incidence of myocardial calcification associated with acute myocardial infarction. *Hum Pathol*. 1989;20:726–731.
 18. Mungro IN, Pagnon J, Kohannim O, Gargalovic PS, Lusis AJ. *cHAC1/MGC4504* is a novel proapoptotic component of the unfolded protein response, downstream of the ATF4-ATF3-CHOP cascade. *J Immunol*. 2009;182:466–476.
 19. Buja LM, Vela D. Cardiomyocyte death and renewal in the normal and diseased heart. *Cardiovasc Pathol*. 2008;17:349–374.
 20. Lefer AM, Tsao P, Aoki N, Palladino MA Jr. Mediation of cardioprotection by transforming growth factor- β . *Science*. 1990;249:61–64.
 21. Bujak M, Frangogiannis NG. The role of TGF- β signaling in myocardial infarction and cardiac remodeling. *Cardiovasc Res*. 2007;74:184–195.
 22. Hermonat PL, Li D, Yang B, Mehta JL. Mechanism of action and delivery possibilities for TGF β 1 in the treatment of myocardial ischemia. *Cardiovasc Res*. 2007;74:235–243.
 23. Jiang Q, Endo M, Dibra F, Wang K, Uitto J. Pseudoxanthoma elasticum is a metabolic disease. *J Invest Dermatol*. 2009;129:348–354.
 24. Nishida H, Endo M, Koyanagi H, Ichihara T, Takao A, Maruyama M. Coronary artery bypass in a 15-year-old girl with pseudoxanthoma elasticum. *Ann Thorac Surg*. 1990;49:483–485.
 25. Schulz V, Hendig D, Szliska C, Gotting C, Kleesiek K. Novel mutations in the *ABCC6* gene of German patients with pseudoxanthoma elasticum. *Hum Biol*. 2005;77:367–384.
 26. Pachori AS, Custer L, Hansen D, Clapp S, Kemppa E, Klingensmith J. Bone morphogenetic protein 4 mediates myocardial ischemic injury through JNK-dependent signaling pathway. *J Mol Cell Cardiol*. 2010;48:1255–1265.
 27. Ye L, Kynaston H, Jiang WG. Bone morphogenetic protein-9 induces apoptosis in prostate cancer cells, the role of prostate apoptosis response-4. *Mol Cancer Res*. 2008;6:1594–1606.
 28. Rajagopal R, Dattilo LK, Kaartinen V, Deng CX, Umans L, Zwijsen A, Roberts AB, Bottinger EP, Beebe DC. Functions of the type I BMP receptor *Acvr1* (*Alk2*) in lens development: cell proliferation, terminal differentiation, and survival. *Invest Ophthalmol Vis Sci*. 2008;49:4953–4960.
 29. Li C, Issa R, Kumar P, Hampson IN, Lopez-Novoa JM, Bernabeu C, Kumar S. CD105 prevents apoptosis in hypoxic endothelial cells. *J Cell Sci*. 2003;116:2677–2685.
 30. Zaidi SH, Huang Q, Momen A, Riaz A, Husain M. Growth differentiation factor 5 regulates cardiac repair after myocardial infarction. *J Am Coll Cardiol*. 2010;55:135–143.
 31. Chen H, Shi S, Acosta L, Li W, Lu J, Bao S, Chen Z, Yang Z, Schneider MD, Chien KR, Conway SJ, Yoder MC, Haneline LS, Franco D, Shou W. BMP10 is essential for maintaining cardiac growth during murine cardiogenesis. *Development*. 2004;131:2219–2231.
 32. Song L, Yan W, Chen X, Deng CX, Wang Q, Jiao K. Myocardial *smad4* is essential for cardiogenesis in mouse embryos. *Circ Res*. 2007;101:277–285.
 33. Chen H, Yong W, Ren S, Shen W, He Y, Cox KA, Zhu W, Li W, Soonpaa M, Payne RM, Franco D, Field LJ, Rosen V, Wang Y, Shou W. Overexpression of bone morphogenetic protein 10 in myocardium disrupts cardiac postnatal hypertrophic growth. *J Biol Chem*. 2006;281:27481–27491.
 34. Puskaric S, Schmitteckert S, Mori AD, Glaser A, Schneider KU, Bruneau BG, Blaschke RJ, Steinbeisser H, Rappold G. *Shox2* mediates *Tbx5* activity by regulating *Bmp4* in the pacemaker region of the developing heart. *Hum Mol Genet*. 2010;19:4625–4633.
 35. Liu J, Stainier DY. *Tbx5* and *Bmp* signaling are essential for proepicardium specification in zebrafish. *Circ Res*. 2010;106:1818–1828.
 36. Takei S, Ichikawa H, Johkura K, Mogi A, No H, Yoshie S, Tomotsune D, Sasaki K. Bone morphogenetic protein-4 promotes induction of cardiomyocytes from human embryonic stem cells in serum-based embryoid body development. *Am J Physiol Heart Circ Physiol*. 2009;296:H1793–H1803.
 37. Choi M, Stottmann RW, Yang YP, Meyers EN, Klingensmith J. The bone morphogenetic protein antagonist noggin regulates mammalian cardiac morphogenesis. *Circ Res*. 2007;100:220–228.
 38. Singh R, Horsthuis T, Farin HF, Grieskamp T, Norden J, Petry M, Wakker V, Moorman AF, Christoffels VM, Kispert A. *Tbx20* interacts with *smads* to confine *tbx2* expression to the atrioventricular canal. *Circ Res*. 2009;105:442–452.
 39. Laflamme MA, Chen KY, Naumova AV, Muskheli V, Fugate JA, Dupras SK, Reinecke H, Xu C, Hassanipour M, Police S, O'Sullivan C, Collins L, Chen Y, Minami E, Gill EA, Ueno S, Yuan C, Gold J, Murry CE. Cardiomyocytes derived from human embryonic stem cells in pro-survival factors enhance function of infarcted rat hearts. *Nat Biotechnol*. 2007;25:1015–1024.
 40. Hao J, Daleo MA, Murphy CK, Yu PB, Ho JN, Hu J, Peterson RT, Hatzopoulos AK, Hong CC. Dorsomorphin, a selective small molecule inhibitor of BMP signaling, promotes cardiomyogenesis in embryonic stem cells. *PLoS One*. 2008;3:e2904.
 41. Kawai T, Takahashi T, Esaki M, Ushikoshi H, Nagano S, Fujiwara H, Kosai K. Efficient cardiomyogenic differentiation of embryonic stem cell by fibroblast growth factor 2 and bone morphogenetic protein 2. *Circ J*. 2004;68:691–702.
 42. Smith KA, Joziassie IC, Chocron S, van Dinther M, Guryev V, Verhoeven MC, Rehmann H, van der Smagt JJ, Doevendans PA, Cuppen E, Mulder BJ, Ten Dijke P, Bakkens J. Dominant-negative *ALK2* allele associates with congenital heart defects. *Circulation*. 2009;119:3062–3069.
 43. Wang J, Sridurongrit S, Dudas M, Thomas P, Nagy A, Schneider MD, Epstein JA, Kaartinen V. Atrioventricular cushion transformation is mediated by *ALK2* in the developing mouse heart. *Dev Biol*. 2005;286:299–310.
 44. Abdalla SA, Letarte M. Hereditary haemorrhagic telangiectasia: current views on genetics and mechanisms of disease. *J Med Genet*. 2006;43:97–110.
 45. Gincul R, Lesca G, Gelas-Dore B, Rollin N, Barthelet M, Dupuis-Girod S, Pilleul F, Giraud S, Plauchu H, Saurin JC. Evaluation of previously unscreened hereditary hemorrhagic telangiectasia patients shows frequent liver involvement and early cardiac consequences. *Hepatology*. 2008;48:1570–1576.
 46. Li Q, Jiang Q, Schurgers LJ, Uitto J. Pseudoxanthoma elasticum: reduced γ -glutamyl carboxylation of matrix gla protein in a mouse model (*Abcc6*^{-/-}). *Biochem Biophys Res Commun*. 2007;364:208–213.
 47. Gheduzzi D, Boraldi F, Annovi G, DeVincenzi CP, Schurgers LJ, Vermeer C, Quagliano D, Ronchetti IP. Matrix Gla protein is involved in elastic fiber calcification in the dermis of pseudoxanthoma elasticum patients. *Lab Invest*. 2007;87:998–1008.
 48. Thomsen SB, Rathcke CN, Zerahn B, Vestergaard H. Increased levels of the calcification marker matrix Gla protein and the inflammatory markers YKL-40 and CRP in patients with type 2 diabetes and ischemic heart disease. *Cardiovasc Diabetol*. 2010;9:86.
 49. Herrmann SM, Whalting C, Brand E, Nicaud V, Garipey J, Simon A, Evans A, Ruidavets JB, Arveiler D, Luc G, Tiret L, Henney A, Cambien F. Polymorphisms of the human matrix gla protein (MGP) gene, vascular calcification, and myocardial infarction. *Arterioscler Thromb Vasc Biol*. 2000;20:2386–2393.
 50. Rider CC, Mulloy B. Bone morphogenetic protein and growth differentiation factor cytokine families and their protein antagonists. *Biochem J*. 2010;429:1–12.